Asian Research Journal of Mathematics

5(2): 1-18, 2017; Article no.ARJOM.31459
ISSN: 2456-477X

Peristaltic Transport with Viscous Dissipation Effect in a Multi-stenosed Artery

W. I. A. Okuyade[1*]

[1]Department of Mathematics and Statistics, University of Port Harcourt, Port Harcourt, Nigeria.

Author's contribution

The sole author designed, analyzed and interpreted and prepared the manuscript.

Article Information

DOI: 10.9734/ARJOM/2017/31459
Editor(s):
(1) Xiao-Jun Yang, Department of Mathematics and Mechanics, China University of Mining and Technology, Xuzhou 221008, China.
Reviewers:
(1) John Abraham, University of St. Thomas, USA.
(2) Jagdish Prakash, University of Botswana, Botswana.
(3) Humaira Yasmin, Majma'ah University, Majma'ah City, Saudi Arabia.
Complete Peer review History: http://www.sciencedomain.org/review-history/19867

Original Research Article

Received: 7th January 2017
Accepted: 9th March 2017
Published: 4th July 2017

Abstract

In this paper, we investigated the effect of pulse amplitude, radius of constriction and Reynolds number on the blood flow through a multi-stenosed artery under the influence of viscous dissipation and insignificant free convective force. The blood flowing through the artery is assumed Newtonian and the artery rigid. The governing nonlinear and coupled partial differential equations are simplified using the stream function and vorticity. The resulting equations are non-dimensionalized and solved by the perturbation series solutions method, as developed by Rao and Devanathan [12]. Analytical expressions are obtained for the flow velocities, pressure and temperature. The effects of the embedded parameters are analyzed quantitatively using graphs. Discussions are considered from a physiologic or clinical point of view. The present model may have some bio-medical applications.

Keywords: Peristaltic transport; viscous dissipation; arterial stenoses; perturbation; vorticity.

1 Introduction

A number of diseases infest the cardiovascular system. Among these is the atherosclerosis of the arteries, which involves the lesion or hardening of the arteries due to deposition of plagues or lipid (a generic term for

**Corresponding author: E-mail: wiaokuyade@gmail.com, wilsonia6011@gmail.com;*

sterols, esters and fats) in the intima (internal walls of the arteries). The sterols cause fribrosis- a thickening and scaring of the connective tissues of the arteries. The local disorders in the process called fibrinolysis leads to the adherence of proteins, fats and blood platelets on the internal walls. The mounting up of these substances gives rise to the formation of constrictions in the channel. The localized atherosclerotic constrictions in the arteries, called stenoses (the narrowing process that causes obstruction to blood flow) [1,2] are noticed mainly in the internal carotid artery, coronary artery and femoral artery, which supplies blood to the brain, cardiac muscles and lower limbs, respectively. [3] Stenosis can occur at the level of the valve or directly below it. And this is regarded as the sub-pulmonary stenosis [4]. The atherosclerotic constrictions serve as blockages to the flow of blood in the arteries. Clinically, the closure of the arteries constitutes a health risk to the patient [5]. The complete closure of the arteries (called atresia) may lead to stroke or heart attack. Even so, moderate and severe stenoses lead to head losses, which can reduce blood supply to the arteries, and imposes an extra load on the heart musculature [3]. In an attempt to maintain the peripheral flow, the heart enlarges itself and also increases the amplitude of the pulse or pressure wave in the arteries [6]. Subsequently, this produces abrupt rise in the flow variables or hydraulic pump, otherwise called shock waves [7]. Furthermore, studies have shown that a stenos artery produces distinct sounds called 'arterial murmurs' or bruits, which can be heard externally. The sounds provide a non-invasive means of detecting patients with carotid artery stenosis [4]. More so, the calcification of these lipids leads to loss of distensibility of the artery at the region of infection, and is assumed rigid. Similarly, the presence of the constriction leads to the evolvement of other geometric forms that change the flow pattern. The plagues may be at one or many points. It may overlap at such points, too. Research workers idealized the evolving new geometries as locally constricted when a point only is affected, and is overlapped [4,8]; peristaltic when many point are plagued and overlapped [9-11].

Rao and Devanathan [12] examined the fluid mechanical aspect of the pulsatile flow of an incompressible viscous fluid through channels of varying cross-sections. They did not consider the roles of other flow characteristics. Therefore, the aim of this study is to examine some of the flow characteristics using the same model and the perturbation series solutions, which they developed.

Much has been done on the pulsating flow in both uniform and varying cross-sectioned non-uniform channels, which in general, approximate the normal and stenosed arteries. [12] investigated the pulsating flow of an incompressible viscous fluid in tubes of varying cross-sections using the perturbation series solutions, which they developed, and found that flow separation occurs in the wall shear stress structure for all geometries; [13] demonstrated the explicit dependence of the overall heat transfer on pulsatile frequency, and found that, for a constant wall temperature boundary condition, the resulting Nusselt number showed periodic axial change, which could enhance heat transfer. [14-16] conducted some experiments on the heat transfer rate, and showed that it increases with pulsatitility. Moreover, [17] solved the Navier–Stokes and the energy equations using a finite difference method and developed an asymptotic series for the dynamic and thermal quantities. Their model shows the existence of an annular effect (Richardson effect) in the entry region for the pulsatile part of the velocity and temperature; [18] studied numerically the pulsating flow in a channel, and concluded that an appreciable heat transfer enhancement occurs in the channel. Likewise, [19] studied the heat transfer in a fully developed pulsatile flow in a channel using numerical method, and noticed that changes in the Nusselt number are predominant in the entrance, but with minor changes in the downstream. They also noticed that oscillation might produce heat transfer enhancement, which may reduce at different axial location in the channel. [20] investigated experimentally, the heat transfer characteristics of a pulsating flow in pipes, and observed that there is a critical frequency at which there is an increase in the steady value of heat transfer for fluids of Prandtl number near unity; for values less than unity the Nusselt number increases as the Prandtl number decreases, whereas the reverse occurs for Prandtl number above unity. [21] examined the thermal effects on the pulsatile flow in tubes with varying cross-section using the vorticity-stream function and perturbation series expansions, and showed that the amplitude of the pulse, height of constriction and Reynolds number of the flow increase the temperature and heat transfer rates in convergent and divergent channels.

Blood is an intelligent fluid that behaves sensitively to geometrical configurations. Therefore, a study of its flow must take cognizance of its peculiar characteristics for which some modeled its flow as Newtonian, and

others non-Newtonian. [22] examined the steady fully developed flow of blood in an atherosclerotic blood vessel with rigid permeable wall, and saw that the increase in the permeability of the blood vessel reduces the resistance due to stenosis. [2] investigated the effects of overlapping stenosis on the flow characteristics of blood under the assumption that blood is Newtonian, and noticed that the impedance increases with the increasing catheter size and stenosis height. [23] considered the oscillatory blood flow in convergent and divergent channels analytically using the perturbation series expansions, and noticed that the increase in the pulse amplitude and height of constriction reduce the axial velocity and axial pressure but increase the radial velocity and wall shear stress; flow separation occurs in the radial velocity and pressure structures in both channels when the height of the constriction is increased. [24] examined analytically the effects of Reynolds number on the oscillating flow in convergent and divergent channels using the method of perturbation series solutions, and observed that increase in the Reynolds number increases the velocities and wall shear stress; a flow separation occurs in the radial velocity flow structure. [25] studied the non-Newtonian effects on Low-Density Lipoprotein transport across an artery using four rheological models, and noticed that non-Newtonian effects on mass transport are negligible for a healthy intramural pressure value; non-Newtonian effects increase slightly with intramural pressure; Newtonian assumption is valid for mass transport at low Reynolds numbers.

The effects of magnetic field on blood flow in diseased arteries have been studied. [1] examined the effect of heat transfer on blood flow in a diseased artery analytically using the closed-form solutions, and found that the height of constriction of the artery, magnetic field and the heat transfer affect the velocity and temperature distributions. The model investigated a stenosed-artery patient under feverish condition. [26] studied the flow of blood in multi-stenosed arteries using a vorticity-stream function and finite difference scheme, and showed that magnetic field modifies the flow patterns, increases the heat transfer rate and the thermal boundary layer thickness. [4] investigated the effect of thermal radiation and magnetic field on the stenosed-arterial blood flow, and observed that magnetic field decreases the blood velocity; the increase in thermal radiation absorption increases the blood temperature. [27] considered analytically the effect of heat and mass transfer on the MHD oscillatory flow in an asymmetric wavy channel in the presence of chemical reaction and heat source using the method of regular perturbation, and found that the heat transport of a system is strongly increased in oscillatory flow than in the ordinary condition.

The geometrical configuration of a flow system has a great influence on the flow patterns. Based on this, a number of research works have been carried out specifically on peristaltic flow. [28] investigated the peristaltic transport of a fluid of variable viscosity under zero Reynolds number and long wavelength approximation, and saw amidst others, that at zero flow rates the pressure rise reduces as the fluid viscosity reduces; the difference between two corresponding values of the pressure rise increases as the amplitude ratio increases; for a given zero pressure rise, the flow rate appreciates as the viscosity of the fluid decreases. [29] studied the peristaltic transport of a non-Newtonian fluid in both uniform and non-uniform channels under zero Reynolds number and long wavelength approximation. Comparing their results with those of the Newtonian fluid model, they observed that at zero flow rate and for a flow behavior index less than one the value of the pressure rise is smaller for the non-Newtonian fluid; at zero flow rate the pressure rise reduces as flow behaviour index drops from one; an increase in the wavelength decreases in pressure rise but increases the non-Newtonian effects. [30] developed an unsteady Newtonian model of blood flow through a multi-stenosed artery in the presence of variable viscosity and body acceleration, and computed the flow patterns for the shear rates and pressure drop. Moreover, [31] studied the peristaltic transport of non-Newtonian fluid in a diverging tube with different wall waveforms using Fourier series, and observed that reflux occurs near the tube wall; the amplitude ratio, power law indices, and shape of the peristaltic waves influences the thickness and shape of the reflux region. [32] developed fluid–solid interaction model of a transient peristaltic transport, and revealed that an increase in the amplitude ratio increases the axial velocity; a rise in the non-Newtonian fluid index reduces the velocity and wall shear stress; the increase in the amplitude of the propagating wave increases the reflux. [33] considered the peristaltic transport of Carreau-Yasuda fluid in a curved channel under the influence of slip condition using a numerical approach, and observed, amongst others, that a rise in the velocity slip parameter reduces the peristaltic flow and weakens the pumping zones; the fluid velocity is higher under the no-slip situation. [34] investigated the electro-kinetically modulated peristaltic transport of non-Newtonian fluids through a narrow confinement

comparable to a deformable tube, and saw that at zero flow rate the viscosity ratio strongly influences the pressure rise; at lower occlusion values the effect of electro-osmosis on the pressure rise is strongly manifested; applied electric field damps the reflux. [35] investigated the effects of homogeneous-heterogeneous reactions on peristaltic transport of third order fluid in a channel with convective boundary conditions in the presence of Hall current and Joule heating using the lubrication approach, and noted that the temperature of the fluid decays due to increase in Biot number. More so, they found that the effects of Hartman number and Hall parameter are quite opposite on temperature profile; the homogeneous and heterogeneous reaction parameters have opposite effects on concentration profile.

Similarly, the effects of plague removal on the arterial blood flow have been investigated. [36] examined the effects of plaque removal (or debulking) in small arteries in a three-dimensional fluid model using experimental and numerical simulation for both Newtonian and non-Newtonian cases, and observed that the removal of the plaque leads to an increase in the rate of blood flow during the systole and diastole streams of the cardiac cycle; the shear stress on the arterial wall is higher for a debulked artery than for a plaque-narrowed one. [37] investigated the time-varying pipe flows driven by a harmonically pulsating inlet velocity using the modified Menter model of numerical simulations, and noticed that the use of a quasi-steady model for the prediction of fully developed friction factors is not applicable for higher frequencies; backflow occurs near the wall as the flow transits from deceleration to acceleration; the amplitudes of the pressure oscillations generated by the imposed velocity variations increase as the frequency increases. [38] investigated the role of plaque removal on blood flow in a popliteal artery using experimental and numerical approaches, and observed that the removal of plaque increases the blood flow rate through the artery; there is a major reduction of pressure loss through the lesion. Even so, [39] studied analytically the transport of Low-Density Lipoprotein through an arterial wall under hyperthermia conditions using a four-layer model, and had results that are in excellent agreement with existing numerical and analytical literature data under isothermal conditions. [40] considered blood flow through arteries under atherectomy situation using an unsteady computational fluid dynamic solver, and found that the atherectomy procedure tends to increase the flow through the stenotic zone.

In this paper, we examine the effects of variation in the amplitude of the pressure wave, height of constriction of the tube, and Reynolds number on the flow characteristics in a peristaltic channel using the asymptotic series expansion developed by [12].

The paper is organized in the following formats: section 2 is the methodology, section 3 holds the results and discussion, and section 4 gives the conclusion.

2 Methodology

We consider the problem of peristaltic transport with viscous dissipation in a multi-stenosed artery. Its formulation is based on the following assumptions: that blood is incompressible and Newtonian, thus allowing the use of the Navier-Stokes equations; arteries are rigid due to the deposition of plagues on them; the viscosity of blood varies with temperature; the plagued arteries are infinite axi-symmetrical cylinders with varying cross-sections; the role of the free convective force is insignificant. More so, we assumed the flow is fully developed and pulsating with a prescribed periodic frequency β and time average volume flux Q at the entrance of the tube. If (X,θ,R) and (u,v,w) are the polar cylindrical orthogonal coordinates and vector components, respectively, assuming the velocity is symmetrical about the θ- axis, the problem becomes two-dimensional with $(X,0,R)$ and $(u,0,w)$. Defining R=0 as the centre or symmetric axis of the tube; $R=a_o(X,t)$, an arbitrary function of X and t as the cross-sectional radius of the tube; a_o as the characteristic radius of the tube, and t as the time, then, the continuity, momentum and energy equations governing the flow are:

$$\frac{\partial u}{\partial X} + \frac{1}{\mathrm{R}}\mathrm{w} + \frac{\partial w}{\partial \mathrm{R}} = 0 \tag{1}$$

$$\frac{\partial \mathrm{u}}{\partial \mathrm{t}}+u\frac{d\mathrm{u}}{\partial X}+w\frac{du}{dR}= \; - \frac{1}{\rho}\frac{\partial p}{\partial X} \; +\upsilon\left(\frac{\partial^2 \mathrm{u}}{\partial \mathrm{X}^2} \; +\frac{\partial^2 \mathrm{u}}{\partial R^2} \; +\frac{1}{R}\frac{\partial u}{\partial R}\right) \tag{2}$$

$$\frac{\partial w}{\partial \mathrm{t}}+\mathrm{u}\frac{\partial w}{\partial \mathrm{X}}+w\frac{\partial w}{\partial \mathrm{R}}=-\frac{1}{\rho}\frac{\partial \mathrm{p}}{\partial \mathrm{R}}+\upsilon\left(\frac{\partial^2 w}{\partial \mathrm{X}^2}+\frac{\partial^2 w}{\partial \mathrm{R}^2}+\frac{1}{\mathrm{R}}\frac{\partial w}{\partial \mathrm{R}}\right) \tag{3}$$

$$\frac{\partial \overline{T}}{\partial t}+u\frac{\partial \overline{T}}{\partial X}+w\frac{\partial \overline{T}}{\partial R}=\frac{k_o}{\rho C_p}\left(\frac{\partial^2 \overline{T}}{\partial R^2}+\frac{1}{R}\frac{\partial \overline{T}}{\partial R}+\frac{\partial^2 \overline{T}}{\partial X^2}\right)+\Phi \tag{4}$$

with the boundary conditions:

$$\text{(i)} \quad \mathrm{w} \; = \; 0, \; \frac{\partial w}{\partial \mathrm{R}}=0, \; \overline{\mathrm{T}}=0 \qquad \text{at} \quad \mathrm{R}=0 \tag{5}$$

(ii) there is no tangential motion at the wall of the tube such that:

$$w(a_o,t)=0\,, \;\; \overline{T}=T_w \;\; \text{at} \;\; R=a_o(X,t) \tag{6}$$

(iii) the cross–sectional flux of the tube is given as:

$$\int_0^{a_o(X,t)} dR\int_0^{2\pi} RUd\theta = 2\pi\psi_o(1+ke^{i\beta t}) \tag{7}$$

where

$$\Phi=\frac{\mu}{\rho C_p}\left[2\left[\left(\frac{\partial w}{\partial R}\right)^2+\left(\frac{w}{R}\right)^2+\left(\frac{\partial u}{\partial X}\right)^2+\left(\frac{\partial w}{\partial X}+\frac{\partial u}{\partial R}\right)^2\right]\right]$$

and is the thermal dissipation function or the rate of dissipation of mechanical energy per unit mass of the fluid due to shear viscosity; ρ is the density; p is the pressure; υ is the kinematic viscosity of the fluid; $\overline{T}$ is the temperature of the fluid; k_o is the thermal conductivity of the arterial wall; C_p is the specific heat capacity at constant pressure of the fluid, and t is the time. ψ_0 is a constant, k is the amplitude of the pulse, which is assumed small, and β is the frequency of oscillation.

For simplicity, we eliminate the pressure terms from equations (2) and (3) by taking the $\frac{\partial}{\partial R}$ of equation (2) and $\frac{\partial}{\partial X}$ of equation (3), then subtracting the first result from the second one, we have

$$\frac{\partial}{\partial t}\left(\frac{\partial u}{\partial R}-\frac{\partial w}{\partial X}\right)+\frac{\partial u}{\partial X}\left(\frac{\partial u}{\partial R}-\frac{\partial w}{\partial X}\right)+\frac{\partial w}{\partial R}\left(\frac{\partial u}{\partial R}-\frac{\partial w}{\partial X}\right)=$$
$$\upsilon\left[\frac{\partial^2}{\partial X^2}\left(\frac{\partial u}{\partial R}-\frac{\partial w}{\partial X}\right)+\frac{\partial^2}{\partial R^2}\left(\frac{\partial u}{\partial R}-\frac{\partial w}{\partial X}\right)+\frac{1}{R}\frac{\partial}{\partial R}\left(\frac{\partial u}{\partial R}-\frac{\partial w}{\partial X}\right)-\frac{1}{R^2}\left(\frac{\partial u}{\partial R}-\frac{\partial w}{\partial X}\right)\right] \tag{8}$$

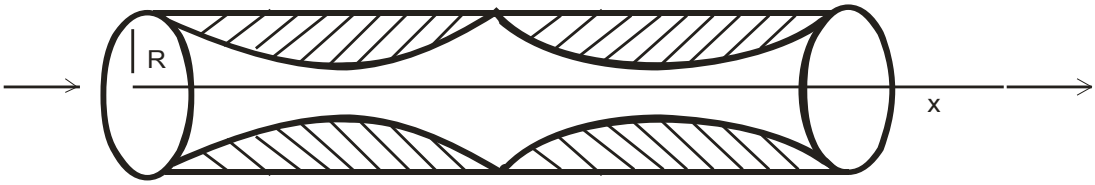

Fig. 1. A physical model of a peristaltic channel

Introducing the stream function ψ, vorticity Ω, respectively i.e.

$$\mathrm{u} = -\frac{1}{R}\frac{\partial \psi}{\partial R},\ \mathrm{w} = \frac{1}{\mathrm{R}}\frac{\partial \psi}{\partial X} \tag{9}$$

$$\Omega = \frac{\partial u}{\partial R} - \frac{\partial w}{\partial X} = \frac{1}{\mathrm{R}}\frac{\partial^2 \psi}{\partial R^2} - \frac{1}{R^2}\frac{\partial \psi}{\partial R} + \frac{1}{R}\frac{\partial^2 \psi}{\partial \mathrm{X}^2} \tag{10}$$

into equations (4) and (8), we have

$$\frac{\partial \Omega}{\partial t} - \frac{1}{R}\frac{\partial \Omega}{\partial X}\frac{\partial \psi}{\partial R} + \frac{1}{R}\frac{\partial \Omega}{\partial R}\frac{\partial \psi}{\partial X} + \frac{\Omega}{R^2}\frac{\partial \psi}{\partial X} = \upsilon\left[\frac{\partial^2 \Omega}{\partial X^2} + \frac{\partial^2 \Omega}{\partial R^2} + \frac{1}{R}\frac{\partial \Omega}{\partial R} - \frac{\Omega}{R^2}\right] \tag{11}$$

$$\frac{\partial \overline{T}}{\partial t} + \frac{1}{R}\frac{\partial \psi}{\partial X}\frac{\partial \overline{T}}{\partial R} - \frac{1}{R}\frac{\partial \psi}{\partial R}\frac{\partial \overline{T}}{\partial X} = \frac{\upsilon}{\mathrm{Pr}}\left[\frac{\partial^2 \overline{T}}{\partial R^2} + \frac{1}{R}\frac{\partial \overline{T}}{\partial R} + \frac{\partial^2 \overline{T}}{\partial X^2}\right] +$$
$$\frac{4\mu}{C_p R}\left[\left(\frac{\partial^2 \psi}{\partial X \partial R}\right)^2 + \frac{1}{R^2}\left(\frac{\partial \psi}{\partial X}\right)^2 - \frac{1}{R}\frac{\partial \psi}{\partial X}\frac{\partial^2 \psi}{\partial X \partial R}\right] +$$
$$\frac{\mu}{C_p R^2}\left[\left(\frac{\partial^2 \psi}{\partial X^2}\right)^2 + \frac{2}{R}\frac{\partial \psi}{\partial R}\frac{\partial^2 \psi}{\partial X^2} - 2\frac{\partial^2 \psi}{\partial X^2}\frac{\partial^2 \psi}{\partial R^2}\right] + \frac{\mu}{C_p R^2}\left[\frac{\partial^2 \psi}{\partial R^2} + \frac{1}{R^2}\frac{\partial \psi}{\partial R} - 2\frac{\partial \psi}{\partial R}\frac{\partial^2 \psi}{\partial R^2}\right] \tag{12}$$

with the boundary conditions as

$$\psi = 0,\ \frac{1}{R}\frac{\partial \psi}{\partial X} = 0,\ \ \frac{1}{R}\frac{\partial^2 \psi}{\partial R^2} - \frac{1}{R^2}\frac{\partial \psi}{\partial R} = 0,\ \ \overline{T} = 0 \quad \text{at} \quad \mathrm{R} = 0 \tag{13}$$

$$\frac{\partial \psi}{\partial R} = 0,\ \ \psi = \psi_o\left(1 + ke^{i\beta t}\right),\ \overline{T} = T_w \ \text{at} \ \ R = a\left(X, t\right) \tag{14}$$

Furthermore, we assume the cross–section of the tube in the model vary in the axial direction, for which we take a (X, t) = $a_o s$ (ε X/a_o , t), $r = R_0(1 + \varepsilon f(x,t))$, $0 \le \mathrm{r} \le 1$ where s is an arbitrary function of x; $0 < \varepsilon = \frac{a_o}{L} << 1$ is a small dimensionless parameter that characterizes the slow variation in the channel radius; a_o is the constant characteristic radius of the tube; L is the characteristic length of the channel, and

$\varepsilon = 0$ corresponds to a tube with constant radius. As ε increases from zero, the variation of ψ in the axial direction depends upon ε x instead of X.

Similarly, introducing the following non-dimensionalized variables

$$r = \frac{R}{a_o}\ , x = \varepsilon \frac{X}{a_o},\ \ \mathrm{T} = \beta \mathrm{t},\ ,\ \phi\ (r, x, T) = \frac{\psi}{\psi_{\mathrm{o}},}\ , \omega(r, x, T) = \frac{\Omega \mathrm{a}_{\mathrm{o}}^{3}}{\psi_{\mathrm{o}}}\ \ , \mathrm{Re} = \frac{\psi_{\mathrm{o}}}{\mathrm{a_o}\nu,}$$

$$\mathrm{Pr} = \frac{k_o}{\rho C_p},\quad \eta = \frac{\beta}{a_o^2 \nu},\ \mathrm{a_o} = \frac{\mathrm{a}}{\mathrm{s}},\quad \Theta = \frac{\overline{T} - T_\infty}{T_w - T_\infty},\ H = \frac{\psi_o^2}{k_o (T_w - T_\infty) a_o^4}$$

where Re is the Reynolds number of the flow, Pr is the Prandtl number, η is a dimensionless number for the frequency of oscillation; T is the dimensionless time; ε is the height of constriction; ϕ, ω and θ are the dimensionless stream function, vorticity and temperature, respectively into equations (10) - (14) respectively, we have

$$\omega = \frac{1}{r}\frac{\partial^2 \phi}{\partial r^2} - \frac{1}{r^2}\frac{\partial \phi}{\partial r} \tag{15}$$

$$\eta \frac{\partial \omega}{\partial T} + \frac{\mathrm{Re}}{r}\varepsilon\left(\frac{\partial \omega}{\partial r}\frac{\partial \phi}{\partial x} + \frac{\partial \omega}{\partial x}\frac{\partial \phi}{\partial r} + \frac{\omega}{r}\frac{\partial \phi}{\partial x}\right) = \frac{1}{r^2}\frac{\partial^2 \omega}{\partial r^2} + \frac{1}{r}\frac{\partial \omega}{\partial r} - \frac{1}{r}\omega \tag{16}$$

$$\eta \frac{\partial \Theta}{\partial T} + \frac{\mathrm{Re\,Pr}}{r}\varepsilon\left(\frac{\partial \phi}{\partial x}\frac{\partial \Theta}{\partial r} - \frac{\partial \phi}{\partial r}\frac{\partial \Theta}{\partial x}\right) = \frac{\partial^2 \Theta}{\partial r^2} + \frac{1}{r}\frac{\partial \Theta}{\partial r} + \frac{H}{r^2}\left[\left(\frac{\partial \phi}{\partial r^2}\right)^2 + \frac{1}{r^2}\left(\frac{\partial \phi}{\partial r}\right)^2 - \frac{2}{r}\frac{\partial \phi}{\partial r}\frac{\partial^2 \phi}{\partial r^2}\right] \tag{17}$$

where the $O(\varepsilon)^2$ terms are neglected for being small.

with the boundary conditions:

$$\phi = 0\ \ ,\ \ \frac{\partial \phi}{\partial x} = 0\ ,\ \ \frac{1}{\mathrm{r}}\ \frac{\partial^2 \phi}{\partial \mathrm{r}^2} - \ \frac{1}{\mathrm{r}^2}\ \frac{\partial \phi}{\partial \mathrm{r}} = 0,\ \Theta = 0 \text{ at } \mathrm{r} = 0 \tag{18}$$

$$\phi = 1\ +\ \mathrm{k\ e}^{\ \mathrm{iT}},\ \frac{\partial \phi}{\partial \mathrm{r}} = 0,\ \Theta = 1 \quad \text{at} \quad \mathrm{r} = \mathrm{s(x,\ T)} \tag{19}$$

Equations (15)-(17) are non-linear and highly coupled. To linearize them, we seek for perturbation series solutions about a small parameter ε. In particular, we use the form developed by [15], which is of the form:

$$f = f^{(o)} + ke^{iT}\overline{f}^{(o)} + \varepsilon\left(f^{(1)} + ke^{iT}\overline{f}^{(1)}\right) + \ldots \tag{20}$$

where f_n represents ω, ϕ and Θ.

Substituting equation (20) into equations (15) – (20), we have:

for zeroth order

$$\omega^{(o)} = \frac{1}{r}\left(\frac{\partial^2 \phi^{(o)}}{\partial r^2} - \frac{1}{r}\frac{\partial \phi^{(o)}}{\partial r}\right) \tag{21}$$

$$\varpi^{(o)} = \frac{1}{r}\left(\frac{\partial^2 \bar{\phi}^{(o)}}{\partial r^2} - \frac{1}{r}\frac{\partial \bar{\phi}^{(o)}}{\partial r}\right) \tag{22}$$

$$\frac{\partial^2 \omega^{(o)}}{\partial r^2} + \frac{1}{r}\frac{\partial \omega^{(o)}}{\partial r} - \frac{1}{r^2}\ \omega^{(o)} = 0 \tag{23}$$

$$\frac{\partial^2 \varpi^{(o)}}{\partial r^2} + \frac{1}{r}\frac{\partial \varpi^{(o)}}{\partial r} - \left(\lambda^2 + \frac{1}{r}\right)\varpi^{(o)} = 0 \tag{24}$$

$$\frac{\partial^2 \Theta^{(o)}}{\partial r^2} + \frac{1}{r}\frac{\partial \Theta}{\partial r} = \frac{-H}{r^2}\left[\left(\frac{\partial^2 \phi^{(o)}}{\partial r^2}\right)^2 + \frac{1}{r^2}\left(\frac{\partial \phi^{(o)}}{\partial r}\right) - \frac{2}{r}\frac{\partial \phi^{(o)}}{\partial r}\frac{\partial^2 \phi^{(o)}}{\partial r^2}\right] \tag{25}$$

$$\frac{\partial^2 \bar{\Theta}^{(o)}}{\partial r^2} + \frac{1}{r}\frac{\partial \bar{\Theta}^{(o)}}{\partial r} - \eta_1 \bar{\Theta}^{(o)} = \frac{-H}{r^2}\left[\frac{\partial^2 \phi^{(o)}}{\partial r^2}\frac{\partial^2 \bar{\phi}^{(o)}}{\partial r^2} + \frac{1}{r^2}\frac{\partial \phi^{(o)}}{\partial r}\frac{\partial \bar{\phi}^{(o)}}{\partial r} - \frac{1}{r}\left(\frac{\partial \phi^{(o)}}{\partial r}\frac{\partial^2 \bar{\phi}^{(o)}}{\partial r^2} + \frac{\partial \phi^{(o)}}{\partial r}\frac{\partial^2 \bar{\phi}^{(o)}}{\partial r^2}\right)\right] \tag{26}$$

where $\lambda^2 = i\eta$

with boundary conditions

$$\left.\begin{aligned} &\phi^{(o)} = \bar{\phi}^{(o)} = 0 \\ &\Theta^{(o)} = \bar{\Theta}^{(o)} = 0 \\ &\frac{1}{r}\frac{\partial \phi^{(o)}}{\partial x} = \frac{1}{r}\frac{\partial \bar{\phi}^{(o)}}{\partial x} = 0 \\ &\frac{\partial}{\partial r}\left(\frac{1}{r}\frac{\partial \phi^{(o)}}{\partial r}\right) = \frac{\partial}{\partial r}\left(\frac{1}{r}\frac{\partial \bar{\phi}^{(o)}}{\partial r}\right) = 0 \end{aligned}\right\} \quad \text{at } r = 0 \tag{27}$$

$$\left.\begin{aligned} \frac{\partial \phi^{(o)}}{\partial r} &= \frac{\partial \bar{\phi}^{(o)}}{\partial r} = 0 \\ \phi^{(o)} &= \bar{\phi}^{(o)} = 1 \\ \Theta^{(o)} &= 1, \bar{\Theta}^{(o)} = 0 \end{aligned}\right\} \quad \text{at} \quad r = s \tag{28}$$

and for the first

$$\omega^{(1)} = \frac{1}{r}\left(\frac{\partial^2 \phi^{(1)}}{\partial r^2} - \frac{1}{r}\frac{\partial \phi^{(1)}}{\partial r}\right) \tag{29}$$

$$\varpi^{(1)} = \frac{1}{r}\left(\frac{\partial^2 \bar{\phi}^{(1)}}{\partial r^2} - \frac{1}{r}\frac{\partial \bar{\phi}^{(1)}}{\partial r}\right) \tag{30}$$

$$\frac{\partial^2 \omega^{(1)}}{\partial r^2} + \frac{1}{r}\frac{\partial \omega^{(1)}}{\partial r} - \frac{1}{r}\omega^{(1)} = \frac{\mathrm{Re}}{r}\left[\frac{\partial \phi^{(o)}}{\partial r}\frac{\partial \omega^{(o)}}{\partial x} + \frac{\partial \phi^{(o)}}{\partial x}\left(\frac{\omega^{(o)}}{r} - \frac{\partial \omega^{(o)}}{\partial r}\right)\right] \tag{31}$$

$$\frac{\partial^2 \varpi^{(1)}}{\partial r^2} + \frac{1}{r}\frac{\partial \varpi^{(1)}}{\partial r} - \left(\lambda^2 + \frac{1}{r^2}\right)\varpi^{(1)} = \frac{\mathrm{Re}}{r}\left[\frac{\partial \phi^{(o)}}{\partial r}\frac{\partial \omega^{(o)}}{\partial x} + \frac{\partial \bar{\phi}^{(o)}}{\partial r}\frac{\partial \omega^{(o)}}{\partial x}\right.$$

$$\left. - \frac{\partial \varpi^{(o)}}{\partial x}\left(\frac{\partial \varpi^{(o)}}{\partial r} - \frac{\varpi^{(o)}}{r}\right) - \frac{\partial \bar{\phi}^{(o)}}{\partial x}\left(\frac{\partial \omega^{(o)}}{\partial r} - \frac{\omega^{(o)}}{r}\right)\right] \tag{32}$$

$$\frac{\partial^2 \Theta^{(1)}}{\partial r^2} + \frac{1}{r}\frac{\partial \Theta^{(1)}}{\partial r} = \frac{\mathrm{Re}\,\mathrm{Pr}}{r}\left[\frac{\partial \phi^{(o)}}{\partial x}\frac{\partial^2 \Theta^{(o)}}{\partial r^2} - \frac{\partial \phi^{(o)}}{\partial r}\frac{\partial \Theta^{(o)}}{\partial x}\right]$$

$$\frac{-2H}{r^2}\left[\frac{\partial^2 \phi^{(o)}}{\partial r^2}\frac{\partial^2 \phi^{(1)}}{\partial r^2} + \frac{1}{r^2}\frac{\partial \phi^{(o)}}{\partial r}\frac{\partial \phi^{(1)}}{\partial r} - \frac{1}{r}\left(\frac{\partial \phi^{(o)}}{\partial r}\frac{\partial^2 \phi^{(1)}}{\partial r^2} + \frac{\partial^2 \phi^{(o)}}{\partial r^2}\frac{\partial \phi^{(1)}}{\partial r}\right)\right] \tag{33}$$

$$\frac{\partial^2\bar{\Theta}^{(1)}}{\partial r^2}+\frac{1}{r}\frac{\partial\bar{\Theta}^{(1)}}{\partial r}-\eta_1{}^2\bar{\Theta}^{(1)}=\frac{\mathrm{Re}\,\mathrm{Pr}}{r}\left[\frac{\partial\phi^{(o)}}{\partial r}\frac{\partial\bar{\Theta}^{(o)}}{\partial r}+\frac{\partial\bar{\Theta}^{(o)}}{\partial x}\frac{\partial\Theta^{(o)}}{\partial r}\;-\frac{\partial\phi^{(o)}}{\partial r}\frac{\partial\bar{\Theta}^{(o)}}{\partial x}-\frac{\partial\bar{\phi}^{(o)}}{\partial r}\frac{\partial\Theta^{(o)}}{\partial x}\right]$$

$$\frac{-2H}{r^2}\left[\frac{\partial^2\phi^{(o)}}{\partial r^2}\frac{\partial^2\bar{\phi}^{(1)}}{\partial r^2}+\frac{1}{r^2}\frac{\partial^2\bar{\phi}^{(o)}}{\partial r^2}\frac{\partial^2\phi^{(1)}}{\partial r^2}-\frac{1}{r^2}\left(\frac{\partial\phi^{(1)}}{\partial r}\frac{\partial\phi^{(o)}}{\partial r}+\frac{\partial\phi^{(o)}}{\partial r}\frac{\partial\bar{\phi}^{(1)}}{\partial r}\right)\mathrm{x}\right.$$
$$\left.-\frac{1}{r}\left(\frac{\partial\phi^{(o)}}{\partial r}\frac{\partial^2\bar{\phi}^{(1)}}{\partial r^2}+\frac{1}{r^2}\frac{\partial\bar{\phi}^{(o)}}{\partial r^2}\frac{\partial^2\phi^{(1)}}{\partial r^2}\right)+\frac{1}{r}\left(\frac{\partial\phi^{(1)}}{\partial r}\frac{\partial^2\bar{\phi}^{(o)}}{\partial r^2}+\frac{\partial\bar{\phi}^{(1)}}{\partial r}\frac{\partial^2\phi^{(o)}}{\partial r^2}\right)\right] \tag{34}$$

with boundary conditions

$$\left.\begin{aligned}&\phi^{(1)}=\bar{\phi}^{(1)}\;=\;0\\&\Theta^{(1)}=\bar{\Theta}^{(1)}\;=\;0\\&\frac{1}{r}\frac{\partial\phi^{(1)}}{\partial x}=\frac{1}{r}\frac{\partial\bar{\phi}^{(1)}}{\partial x}\;=0\\&\frac{\partial}{\partial r}\left(\frac{1}{r}\frac{\partial\phi^{(1)}}{\partial r}\right)=\frac{\partial}{\partial r}\left(\frac{1}{r}\frac{\partial\bar{\phi}^{(1)}}{\partial r}\right)=\;0\end{aligned}\right\}\quad\text{at r = 0} \tag{35}$$

$$\left.\begin{aligned}&\frac{\partial\phi^{(1)}}{\partial r}=\frac{\partial\bar{\phi}^{(1)}}{\partial r}\;=0\\&\phi^{(1)}=\bar{\phi}^{(1)}=0\\&\Theta^{(1)}=\bar{\Theta}^{(1)}=0\end{aligned}\right\}\quad\text{at}\quad\text{r = s} \tag{36}$$

The solution of the zeroth order equations (21) - (28) are:

$$\phi^{(o)}=2\left(\frac{r}{s}\right)^2-\left(\frac{r}{s}\right)^4+\ldots \tag{37}$$

$$\bar{\phi}^{(o)} = \quad + \frac{2}{\lambda s^2 I_2(\lambda s)}\left[I_o(\lambda s) - I_o(\lambda r) + I_2(\lambda r)\right]\frac{r^2}{2} + \ldots \tag{38}$$

$$\omega^o = -\frac{8}{s^3}\left(\frac{r}{s}\right) + \ldots \tag{39}$$

$$\bar{\omega}^{(O)} = -2\frac{\lambda I_1(\lambda r)}{s^2 I_2(\lambda s)} + \ldots \tag{40}$$

$$\Theta^{(o)} = 1 + \frac{4H}{s^4}\left[1 + \left(\frac{r}{4}\right)^4\right] + \ldots \tag{41}$$

$$\bar{\Theta}^{(o)} = \frac{-16H}{s^6 I_2(\lambda s)}\left[\left(\frac{r^2}{5} - \frac{s^2}{5} + \frac{\lambda s}{15}\frac{I_1(\lambda s)}{I_o(\lambda s)}\right)I_o(\lambda r) + \frac{\lambda r I_1(\lambda s)}{15}\right] \tag{42}$$

while those of the first order equations (29) - (36) are:

$$\phi^{(1)} = -\frac{\mathrm{Re}}{s}\frac{\partial s\varepsilon}{\partial x}\left[\frac{1}{9}\left(\frac{r}{s}\right)^8 - \frac{2}{3}\left(\frac{r}{s}\right)^6 + \left(\frac{r}{s}\right)^4 - \frac{4}{9}\left(\frac{r}{s}\right)^2 + \ldots\right] \tag{43}$$

$$\bar{\phi}^{(1)} = \frac{4\,\mathrm{Re}}{\lambda^4 s^4}\frac{\partial s}{\partial x}\left\{\frac{I_1(\lambda r)}{s\lambda^2 I_2(\lambda s)}\left[\left(\frac{2}{3}s^4\lambda^4 - 5s^2\lambda^2 - 32\right)\lambda I_1^2(\lambda s)\right.\right.$$

$$+\left(\frac{1}{2}s^2\lambda^2 + 16\right)\lambda^2 s I_o(\lambda s) I_1(\lambda s) + \left(\frac{2}{3}\lambda^4 s^4 + 12\lambda^2 s^2 - 128\right)\frac{I_1(\lambda s)}{s}$$

$$\left.\left.+\left(64 - 6\lambda^2 s^2 - \frac{1}{4}\lambda^4 s^4\right)\lambda I_o(\lambda s)\right] + \ldots\right\} \tag{44}$$

$$\omega^{(1)} = \frac{8\,\mathrm{Re}}{s^4}\frac{\partial s}{\partial x}\left[\frac{2}{3}\left(\frac{r}{s}\right)^5 - 2\left(\frac{r}{s}\right)^3 + \left(\frac{r}{s}\right)\right] + \ldots \tag{45}$$

$$\bar{\omega}^{(1)} = 4\frac{\mathrm{Re}}{\lambda^4 s^4}\frac{\partial s}{\partial x}\left\{\frac{1}{\lambda^2 I^2(\lambda s)}\left[\left(\frac{2s^4\lambda^4}{3} - 5s^2\lambda^2 - 32\right)\lambda I_1^2(\lambda s) + \ldots\right]\right.$$

$$\left.+\left[I_o(\lambda r)\left(\lambda s^2 r - \frac{\lambda r^2}{3}\right)I_1(\lambda s) - \frac{r^3}{s} + 2sr\right] + \ldots\right\} \tag{46}$$

$$\Theta^{(1)} = \frac{\mathrm{Re}\,H}{9s^5}\frac{\partial s}{\partial x}\left(20-101\,\mathrm{Pr}\right)+\frac{64\,\mathrm{Re}\,\mathrm{Pr}\,H}{s^9}\frac{\partial s}{\partial x}\left(\frac{r^2}{4}-\frac{r^4}{16s^2}-\frac{r^6}{36s^4}-\frac{r^8}{64s^6}\right)$$

$$+128\frac{\mathrm{Re}\,H}{s^9}\frac{\partial s}{\partial x}\left(\frac{r^4}{16}-\frac{r^6}{18s^2}-\frac{r^8}{96s^4}\right) \tag{47}$$

$$\bar{\Theta}^{(1)} = \frac{32\,\mathrm{Re}}{s^{11}I_2^2(\lambda s)}\frac{\partial s}{\partial x}\left[\left(\frac{2}{3}s^4\lambda^4-5s^2\lambda^2-32\right)I_1^2(\lambda s)+\left(\frac{1}{2}s^2\lambda^2+16\right)\lambda s I_o(\lambda s)\right.$$

$$\left.+\left(\frac{3}{2}s^4\lambda^4-12s^2\lambda^2-128\right)\frac{I_1(\lambda s)}{\lambda s}+\left(64-6s^2\lambda^2-\frac{1}{4}s^4\lambda^4\right)I_o(\lambda s)\right]\mathrm{x}$$

$$\left[\frac{r^2}{5}I_o(\lambda r)-\frac{\lambda r}{15}I_1(\lambda r)-\frac{s^2}{5}I_o(\lambda s)+\frac{\lambda s}{15}I_1(\lambda s)\right] \tag{48}$$

where I_o (λr), I_1(λr), I_2 (λr), I_o(λs), I_1(λs) and I_2 (λs) are the modified Bessel function of order zero, one, and two, respectively. It is worthy to note that equations (44) and (46) are developed from [12] solutions, p. 206.

3 Results and Discussion

The model in Fig. 1 shows the transport of blood through a peristaltic channel, an idealized multi-stenosed artery. We examined the flow characteristics in the channel. The problem shows that the flow structure depends mostly on the variations in the amplitude of the pulse wave, height of constriction and Reynolds number. Figs. 2–6 show the profiles of the computational results for the axial pressure, radial and axial velocities and temperature for various values of the amplitude (k), height of constriction (ε) and Reynolds number (Re). The computation was done with Maple 12 computational software. For realistic constant values of H(x)=1; Pr=0.7; T=π/4; λ=2, and varied values of k = 0.01, 0.03, 0.05, 0.07; ε = 0.01, 0.03, 0.05, 0.07; Re= 10, 100, 500, 1000 the profiles show that the

- Increase in the amplitude decreases the axial pressure, axial and radial velocities, and temperature;
- Increase in the height of constriction increases the axial pressure but decreases the axial and radial velocities, and temperature;
- Increase in the Reynolds number tends to decrease the axial and radial velocities and temperature but has no significant effect on the pressure.

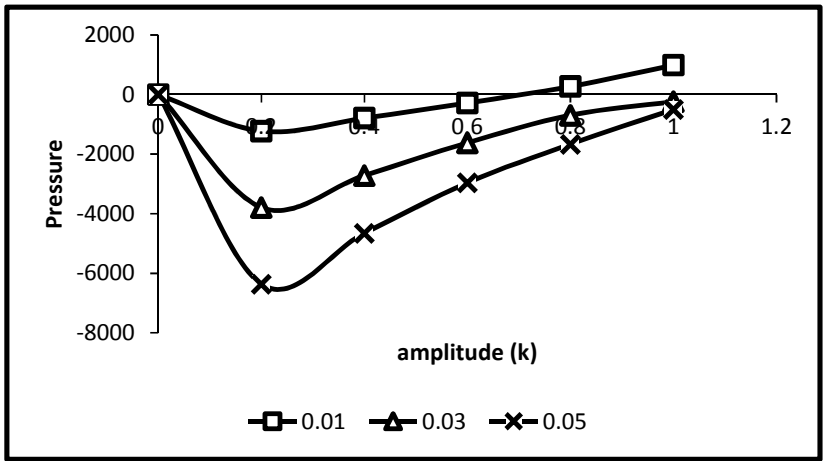

Fig. 2. Pressure–amplitude (k) profiles

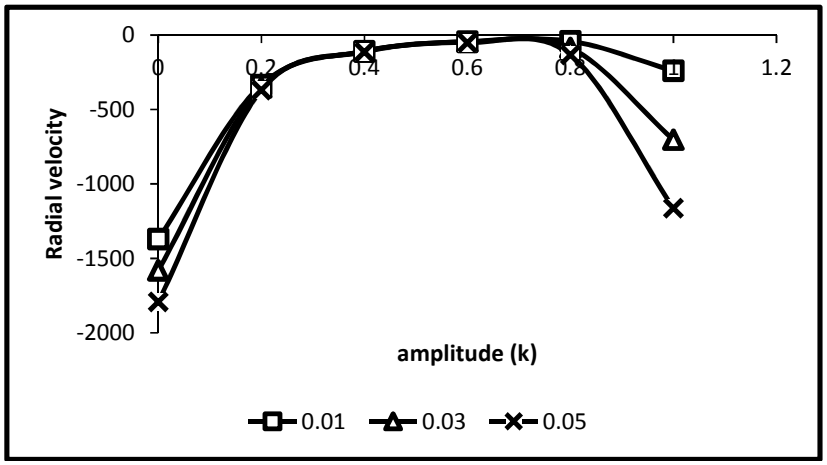

Fig. 3. Radial velocity–amplitude (k) profiles

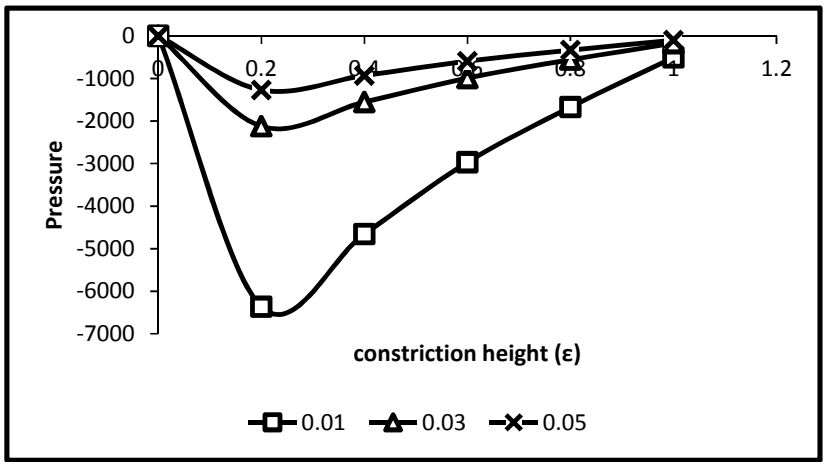

Fig. 4. Pressure-height of constriction (ε) profiles

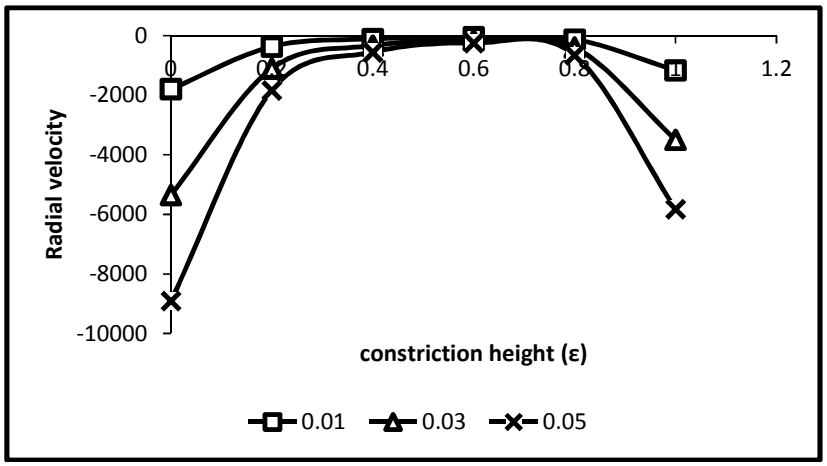

Fig. 5. Radial velocity-height of constriction (ε) profiles

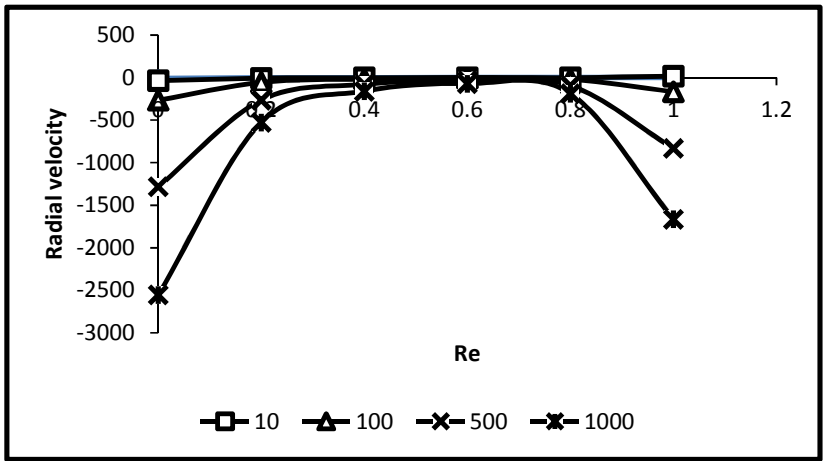

Fig. 6. Radial velocity-Reynolds number (Re) profiles

In a normal artery, blood flow is laminar, Poiseuille and fully developed. But due to stenoses, the arterial channel is blocked either moderately or severely. For this, the heart enlarges itself to maintain peripheral flow. The enlargement of the heart leads to an increase in the amplitude of the pulse or pressure wave. More so, the increase in the amplitude empowers the flow variables in the direction of the increase, which in this case, is in the radial direction. An increase in the pulse wave gives rise to an increase in the size of the amplitude, which consequently, increases the strength of the flow variables in that direction. In extreme cases, this leads to abrupt rise in the flows variables, otherwise called shocks. However, the result in Fig. 3 shows that the radial velocity decreases as the amplitude increases. This is a negative result. Possibly, it could be due to the effect of geometric configuration of the channel. On the other hand, the increase in the amplitude of the pulse wave will reduce the strength of flow variables in the axial direction, as seen in Fig. 2. This result strongly agrees with [23], though a case of convergent and divergent channels.

As said above, the arterial blood flow is laminar, Poiseuille and fully developed. The arterial blood moves with the velocity with which it is released from the heart. As it approaches the region of the constriction, the flow pattern changes. Moreover, the rise in the constriction height determines the channel configuration, size of the available opening at the point of the plague, and the flow axial pressure situation. The overall analysis shows that the increase in the height of constriction increases the axial pressure (see Fig. 4) but decreases the radial velocity (see Fig. 5).

Similarly, in the upstream, that is, the region before the plague, the flow is laminar and Poiseuille, therefore; its Reynolds number is moderate. However, towards the peak of the constriction, that is, in the convergent section whose geometry rises exponentially, the inertial force rises and consequently, the Reynolds number and the momentum rise. On the other hand, in the divergent section whose geometry enlarges exponentially from the peak, the inertial force drops. This must be followed by a drop in the Reynolds number and momentum. Subsequently, the flow variables must drop. The weakened flow variables here may not rise in the next convergent section of the channel. Consequent upon this, the strength of the flow variables may be on the downward trend. This could account for what is seen in the radial velocity (Fig. 6). This is also a negative report.

The drop in the pressure and velocity has some complex physiologic, clinical or health implications on the patient. The arteries are the vehicles through which nutrients are conveyed to other parts of the body. Therefore, the drop in the pressure and velocity levels of the flow reduces their availability in the body, which may lead to cell starvation.

4 Conclusion

We considered the peristaltic transport with viscous dissipation effect through a multi-stenosed artery.

The analyses of results show that an increase in the amplitude decreases the axial pressure and radial velocity; an increase in the height of constriction increases the axial pressure but decreases the radial velocity; an increase in the Reynolds number decreases the radial velocity but has no significant effect on the axial pressure. This study tends to report negative results. Furthermore, it is observed that the reduction in pressure and velocity has some attendant clinical implications on the atherosclerotic patient.

Competing Interests

Author has declared that no competing interests exist.

References

[1] Ogulu A, Abbey TM. Simulation of heat transfer on an oscillatory blood flow in an indented porous artery. International Communications in Heat and Mass Transfer. 2005;32:983–989

[2] Srivastava VP, Rochana Vishnoi, Dharmendra Singh, Amit Medhavi, Shailesh Mishra. Response to blood flow through an overlapping stenosis in catheterized arteries. e-Journal of Science and Technology. 2011;5(6):93-103.

[3] Mittal R, Simmons SP, Najjar F. Numerical study of pulsatile flow in a constricted channel. Journal of Fluid Mechanics. 2003; 485:37-378.

[4] Prakash J, Makinde OD. Radiative heat transfer to blood flow through a stenotic artery in the presence of magnetic field. Latin American Applied Research. 2011; 41:273-277.

[5] Nichol WW, O'Rourke MF. McDonald's blood flow in arteries. Theoretical, Experimental and Clinical Principles. 4th Edition. Oxford University Press; 1998.

[6] Aniliker M, Rockwell RL, Ogden E. Nonlinear analysis of pulses and shock waves in arteries, II. Z. Angnew Mathematics and Physics. 1971; 22:563-581.

[7] Ayeni RO, Akinrelere EA. On temperature factor and effect of viscosity on blood temperature in the arteries. Journal of Theoretical Biology. 1984; 109:479-487.

[8] Lee JS, Fung YC. Flow of incompressible fluid in locally constricted tubes. Journal Applied Mechanics. 1970; 37:9.

[9] Burns JC, Parkes T. Flow of an incompressible fluid in peristaltic tubes. Journal of Fluid Mechanics. 1967; 29:731.

[10] Shapiro AH, Jaffin MY, Weinburg SL. Flow of incompressible fluid in peristaltic tubes. Journal of Fluid Mechanics. 1969; 37:409.

[11] Yih FC, Fung YC. Flow of incompressible fluid in peristaltic tubes. Journal of Applied Mechanics. 1971;47:93.

[12] Rao AR, Devanathan R. Pulsatile flows in tubes of varying cross-sections. Z. Angew Mathematics and Physics. 1973; 24:203-213.

[13] Siegel R, Perlmutter. Heat transfer for pulsating laminar duct flow. Trans ASME Journal Mathematics and Physical Sciences. 1962; 26:19-36.

[14] Fallen M. Heat transfer in a pipe with superimposed pulsating flow. Wameund Stolffubertragun. 1982;16:89-99.

[15] Peattle R, Budwig R. Heat transfer in laminar oscillating flow in cylindrical and conical tubes. International Journal of Heat Mass Transfer. 1989;32(5):923-934.

[16] Gernin LG, Manchikha SP, Loval AP, Sviridov VG. Hydrodynamics and heat transfer with pulsating fluid flow in tubes. Thermal Engineering. 1993;39.

[17] Creff R, Andrew P. Dynamic and convective results from a developing unsteady flow. International Journal of Numerical Methods in Fluids. 1985;5:745-760.

[18] Haneke H, Laschelfski H, Grobe-Gergemann A, Mitra NK. Natural forced convection and combustion simulation. Advanced Computer Methods in Heat Transfer. 1992;11(2):287-298.

[19] Kim YC, Kang BH, Hyun JM. Heat transfer in thermally developing region of a pulsating channel flow. International Journal of Heat Mass Transfer. 1993;36(17):425-426.

[20] Base TE, Campbel MR, Hobbs J. The effect of a pulsating flow on the forced convection heat transfer inside a circular heated tube. Process 15th Canadian Congress of Applied Mechanics, Cancam. 1995; 95(2):612-613.

[21] Okuyade WIA, Mbeledogu IU, Abbey TM. Heat transfer effects on pulsatile flow in tubes with slowly varying cross-sections, Asian Journal of Applied Sciences. 2015; 3(6):770–783.

[22] Das B, Batra RL. Non-Newtonian flow of blood in atherosclerotic blood vessel with rigid permeable walls. Journal of Theoretical Biology. 1995;175:1–11.

[23] Okuyade WIA, Abbey TM. Oscillatory blood flow in convergent and divergent channels, Part 1: Effects of pulse amplitude and local constriction height. British Journal of Mathematics and Computer Science. 2016;14(6):1-17.

[24] Okuyade WIA, Abbey TM. Oscillatory blood flow in convergent and divergent channels, Part 2: Effects of Reynolds number. British Journal of Mathematics and Computer Science. 2016;15(1):1-14.

[25] Marcello Iasiello, Kambiz Vafai, Assunta Andreozzi, Nicola Bianco. Analysis of non-Newtonian effects on low-density lipoprotein accumulation in an artery. Journal of Biomechanics. 2016;49(9):1437-1446.
DOI: http://dx.doi.org/10.1016/j.jbiomech.2016.03.017

[26] Bourhan Tashtoush, Ahmad Magableh. Magnetic field effect on heat transfer and fluid flow characteristics of blood flow in multi-stenosis arteries. Journal of Heat Mass Transfer. 2008;44:297–304.
DOI: 10.1007/s00231-007-0251-x

[27] Satya Narayana PV, Venkateswarlu B, Devika B. Chemical reaction and heat source effects on MHD oscillatory flow in an irregular channel. Ain Shams Engineering Journal; 2015. - (in press).

[28] Srivastava LM, Srivastava VP, Sinha SN. Peristaltic transport of a physiological fluid. Part-I. Flow in non-uniform geometry. Biorheology. 1988;20(2):53-66.

[29] Srivastava LM, Srivastava VP. Peristaltic transport of a non-Newtonian fluid: Applications to the vas deferens and small intestine. Annals of Biomedical Engineering. 1985;13(2):137-153.
DOI: 10.1007/BF02584235

[30] Chakravarty S, Sannigrahi A. A nonlinear mathematical model of blood flow in a constricted artery experiencing body acceleration. Mathematical Computational Modeling. 1999;29:9–25.

[31] Prasanna Hariharan, Seshadri V, Rupak K. Banerjee. Peristaltic transport of non-Newtonian fluid in a diverging tube with different wave forms. Mathematical and Computer Modeling. 2008;48(7,8):998–1017.
DOI: 10.1016/j.mcm.2007.10.018

[32] Kohyar Y, Hanieh N. New approach in modeling peristaltic transport of non-Newtonian fluid. Journal of Mechanics and Medical Biology. 2013;13(1350052).
DOI: 101142\S0219413500528

[33] Tasawar Hayat, Fahad Munir Abbasi, Bashir Ahmad, Ahmed Alsaedi. Peristaltic transport of Carreau-Yasuda fluid in a curved channel with slip effects. PLoS ONE. 2014;9(4):e95070.
DOI: http://dx.doi.org/10.1371/journal.pone.0095070

[34] Goswami P, Chakraborty J, Bandopadhyay. Electrokinetically modulated peristaltic transport of power-law fluids. Microvasc Research; 2016.
DOI: 10.1016/j.mvr.2015.10.004. [41] M

[35] Hayat T, Aneela Bibi, Humaira Yasmin, Ahmad B. Simultaneous effects of Hall current and homogeneous/heterogeneous reactions on peristalsis. Journal of the Taiwan Institute of Chemical Engineers.2016; 58:28–38.
DOI: http://dx.doi.org/10.1016/j.jtice.2015.05.037

[36] Abraham JP, Sparrow EM, Lovik RD. Unsteady three-dimensional fluid mechanic analysis of blood flow in plaque-narrowed and plaque-freed arteries. International Journal of Heat and Mass Transfer; 2008.

[37] Gebreegziabher T, Sparrow EM, Abraham JP, Ayorinde E, Singh T. High-frequency pulsatile pipe flows encompassing all flow regimes. Numerical Heat Transfer; Part A: Applications. 2011;60(10): 811-826.
DOI: 10.1080/10407782.2011.627794

[38] Brian Plourde D, Lauren Vallez J, Biyuan Sun, John Abraham P, Cezar Staniloe S. The effect of plaque Removal on pressure drop and flow rate through an idealized stenotic lesion. Biology and Medicine; 2015.
DOI: http://dx.doi.org/10.4172/0974-8369.1000261

[39] Marcello Iasiello, Kambiz Vafai, Assunta Andreozzi, Nicola Bianco. Low-density lipoprotein transport through an arterial wall under hyperthermia and hypertension conditions – An analytical solution. Journal of Biomechanics; 2015.
DOI: http://dx.doi.org/10.1016/j.jbiomech.2015.12.015

[40] Plourde BD, Vallez LJ, Sun B, Nelson-Cheeseman BB, Abraham JP, Staniloae CS. Alterations of blood flow through arteries following atherectomy and the impact on pressure variation and velocity. Cardiovasc. Eng. Technol. 2016; 7(3):280-289.
DOI: 10.1007/s13239-016-0269-7

Peer-review history:
The peer review history for this paper can be accessed here (Please copy paste the total link in your browser address bar)
http://sciencedomain.org/review-history/19867